How to cite: *Angew. Chem. Int. Ed.* **2024**, *63*, e202404682
doi.org/10.1002/anie.202404682

Supramolecular Chemistry

Shape-Complementary Multicomponent Assembly of Low-Symmetry Co(III)Salphen-Based Coordination Cages

*Bo Zhang, Haeri Lee, Julian J. Holstein, and Guido H. Clever**

Dedicated to Prof. Dr. Thomas J. J. Müller on the occasion of his 60th birthday

Abstract: While metal-mediated self-assembly is a popular technique to construct discrete nanosized objects, highly symmetric structures, built from one type of ligand at a time, are dominating reported systems. The tailored integration of a set of different ligands requires sophisticated approaches to avoid narcissistic separation or formation of statistical mixtures. Here, we demonstrate how the combination of three structure-guiding effects (metal-templated macrocyclization, additional bridging ligands and shape-complementarity) based on Co(III)salphen metal nodes allows for a rational and high-yielding synthesis of structurally complex, lantern-shaped cages with up to four differentiable bridges. Three new heteroleptic coordination cages based on dinuclear Co(III)salphen macrocycles were synthesized in a one-pot reaction approach and fully characterized, including single crystal X-ray analyses. One cage groups two of the same ligands, another two different ligands around a symmetric Co_2-bis-salphen ring. In the most complex structure, this ring is unsymmetric, rendering all four connections between the two metal centers distinguishable. While heteroleptic assembly around Pd(II) nodes has been shown to be dynamic, beneficial for cage-to-cage transformations, assembly cascades and adaptive systems, the herein introduced cages based on kinetically more inert Co(III)salphen will be advantageous for applications in enzyme-like catalysis and molecular machinery that require enhanced structural and chemical stability.

Introduction

Most molecular recognition and catalytic transformation processes in biological systems take place in nanosized cavities. Synthetic supramolecular chemistry attempts to mimic such confined environments within porous materials or discrete cages based on organic linkages or coordination chemistry. The dynamic, metal-mediated self-assembly of organic bridging ligands and metal cations with a defined coordination geometry has developed into a reliable and robust approach to construct a large variety of discrete, soluble objects and solid-state materials.[1–6] In most reported examples, a single type of ligand, with its specific geometry and denticity, is employed, yielding highly symmetric structures such as rings,[7–9] lantern-shaped cages[10,11] or shapes derived from Platonic, Archimedean or Goldberg polyhedra.[12–21] Despite their mathematically touching beauty and straightforward, often quantitative formation, there are only few biological structures with an accessible interior, such as virus capsids and iron storage proteins, that actually resemble these highly symmetric artificial architectures. Most nano-sized cavities of biological origin are highly asymmetric and equipped with several different functional moieties. The rational construction and high-yielding assembly of low-symmetric nano-confinements, however, is challenging, in particular when a high structural and chemical stability is targeted. Sequential covalent organic synthesis towards such nano-confinements is difficult to apply in a modular fashion and only few reports address the problem using (dynamic) covalent approaches[22–25] or multicomponent reactions.[26] While metal-mediated self-assembly allows for a rapid diversification of individual ligand-metal combinations, the rational integration of a set of different ligands into the same architecture bears the risk of narcissistic self-sorting or the formation of entropically driven product mixtures with a statistical distribution of components.[27,28] Recently, a number of coordination architectures containing two different organic ligands in determined positions have been reported.[29] Some examples are based on specific secondary interactions between neighboring ligands or ligands and guests. Nitschke and co-workers reported integrative self-sorting driven by π-stacking between different ligands,[30–32] Yoshizawa obtained heteroleptic host–guest complexes templated by C_{60},[33] and Crowley exploited ligand-to-ligand hydrogen bonding by introducing amino groups close to the donor site.[34] Further approaches make use of coordination sphere engineering (CSE) where elec-

[*] Dr. B. Zhang, Dr. J. J. Holstein, Prof. Dr. G. H. Clever
Department of Chemistry and Chemical Biology, TU Dortmund University, Otto-Hahn-Strasse 6, 44227 Dortmund (Germany)
E-mail: guido.clever@tu-dortmund.de
Prof. Dr. H. Lee
Department of Chemistry, Hannam University, 1646 Yuseong-daero, Yuseong-gu, Daejeon 34054, Republic of Korea

tronic complementarity between *trans*-standing ligands is employed or steric bulk is introduced to shape a heteroleptic coordination environment. Stang et al. pioneered the electronic route[35] while Fujita exploited the combination of bulky lutidines and lean pyridines around *cis*-protected [Pd(en)] fragments to assemble rectangles and prismatic cages.[36,37] We recently expanded this principle by grouping bulky donors around 'naked' Pd(II) centers, yielding heteroleptic *cis*-[38] and *trans*-[$Pd_2L_2L'_2$][39] as well as unique 1+3 two-component [$Pd_2LL'_3$] cages.[39–43] Ribas, Reek and coworkers generated heteroleptic cuboids by saturating metallo-macrocycles with bridging ligands.[44] Finally, shape-complementary assembly (SCA) between matching ligand scaffolds has been employed by Fujita,[45] Nitschke,[46] Mukherjee,[47,48] Chand,[49] Zhou,[50] Sun[51] and us[52,53] to construct various two-ligand assemblies with a defined structure. However, very few examples exist where integrative, metal-mediated self-sorting into a single product was achieved from three or more organic components. Noteworthy, Schmittel has driven the complexity of self-assembled rings and cages to an impressive level by using extensively engineered donor combinations.[54,55]

Combining more than two different ligands around two naked Pd(II) nodes turned out to be very challenging.[40,56–61] In principle, the combination of four different, but equally shaped, bis-monodentate ligands **A**, **B**, **C** and **D**, similarly able to fill the four positions that bridge two square-planar metal centers, gives rise to the formation of 55 different species, from the homoleptic combinations, e.g. [$Pd_2\mathbf{A}_4$], to the most complex multicomponent product (Figure 1a). Selectively obtaining the integratively self-sorted assembly of maximal complexity, [Pd_2**ABCD**], has been recently achieved by Hiraoka[60] and us[61] under kinetic or thermodynamic control, respectively.

Owing to their pronounced structural dynamicity, kinetically labile Pd(II)-mediated cages are of high relevance for realizing stimuli-responsive, complex systems or self-sorting cascades.[42,59,62] On the other hand, some application areas benefit from a higher structural and chemical stability, achievable by the use of more inert coordination environments. While going from Pd(II) to Pt(II) might be an obvious choice, the latter metal has mainly found entry into multicomponent macrocycle chemistry[63] but its use in the clean and high-yielding realization of heteroleptic coordination cages has not yet been reported. Alternatively, transition metal ions where ligand exchange kinetics can be controlled via a redox process, such as in the pair Co(II)/Co(III) offer great potential to be used in non-statistical multicomponent assembly.[64]

We herein introduce the modular synthesis of a series of Co(III)-mediated cages by combining three approaches within a single synthetic strategy: 1) closure of an unsymmetric Co_2-bis-salphen macrocycle via precondensation of one bridge with *ortho*-phenylene diamine, templated by cobalt coordination, 2) saturation of this metallo-macrocycles via the installation of two bis-pyridyl bridges to generate a 3D cavity and 3) shape-complementarity between the latter two ligands resulting in bridge-differentiation (Figure 1b–c). On the way to solving this puzzle, we created a network of combinations in which five different organic bridges can be combined with each other and Pd(II) or Co(II) cations (oxidized to kinetically inert Co(III) centers along the way) to selectively form five different coordination cages, four of which are heteroleptic (Figure 2).

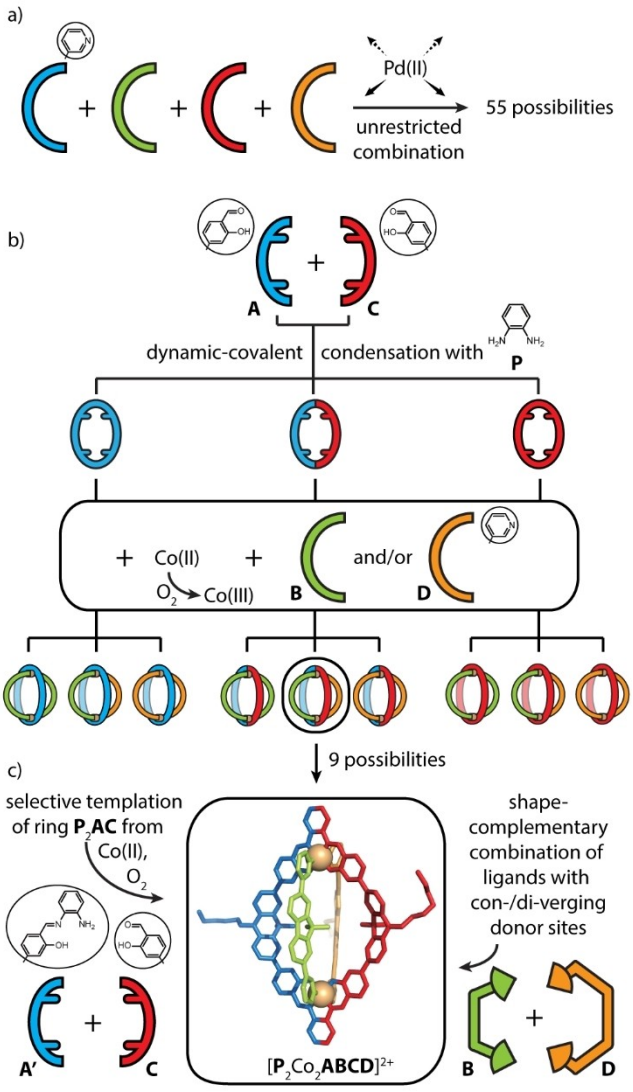

Figure 1. Heteroleptic assembly of dinuclear lantern-shaped cages. a) Statistical outcome expected for four different banana-shaped, bis-monodentate ligands of equal shape and two square-planar cations, leading to a maximum of 55 possible products (see Supporting Information); b) restriction to nine possible products by construction of a bis-salphen macrocycle from two bifunctional salicylic aldehydes plus *ortho*-phenylene diamine (**P**), cobalt complexation and coordination of two equally shaped bis-pyridyl bridges; c) further restriction to one product [P_2Co_2**ABCD**] by cobalt-templated desymmetrization of the bis-salphen macrocycle and completion of the heteroleptic cage with two shape-complementary bis-pyridyl ligands (in compound naming schemes, **A**, **B**, **C** and **D** refer to the different bridges; in cages, component **P** is named in front of the cobalt ion for the sake of clarity).

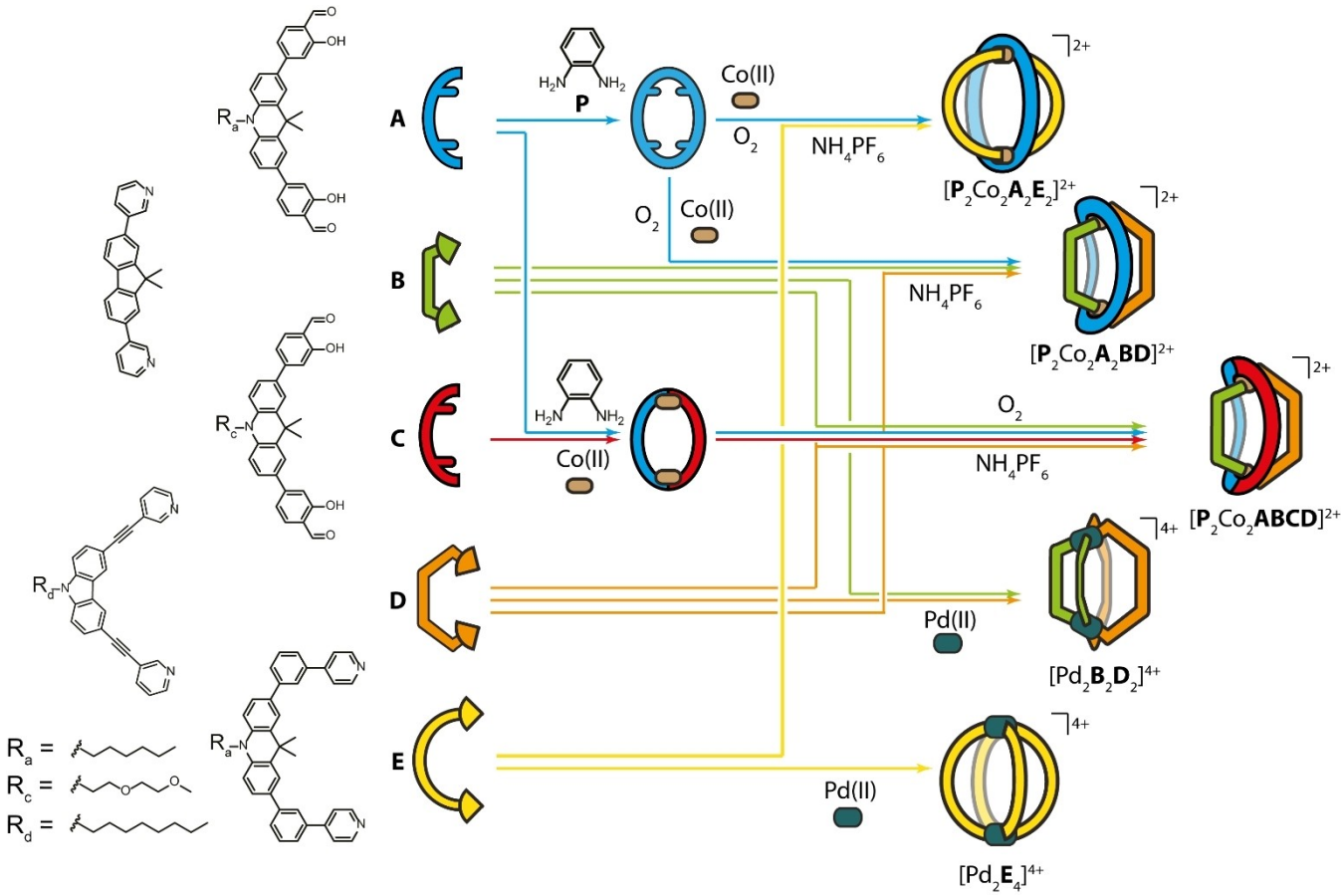

Figure 2. Modular coordination cage assembly scheme. Construction of homo- and heteroleptic [M_2L_4] cages via the following approaches: bis-salphen macrocyclization (blue arrow), ring-desymmetrization via metal-templation (blue/red), saturation of macrocycles with two bridges (first three cages) and bridge-differentiation via shape-complementarity (second to fourth cage).

Results and Discussion

En route to the final goal of combining four different bridges within one lantern-shaped structure, we evaluated a series of ligand geometries and chemistries, metal centers and combinations of assembly principles. In the following, we report the stepwise increase of structural complexity, resulting from a close interplay between computer-aided molecular design and experiment-based results, yielding five members of a family of four-stranded homo- and heteroleptic cages in a predictive way. All newly obtained structures were comprehensively analyzed by 2D NMR techniques, mass spectrometric methods and single crystal X-ray diffraction using synchrotron radiation.

Heteroleptic cage $[P_2Co_2A_2E_2]^{2+}$

Previously, we succeeded in combining two different ligands with square-planar Pd(II) cations in *cis*-configured [$Pd_2L_2L'_2$] assemblies by either using donor site engineering[38] or shape-complementary[52,53] but realized that the rational combination of three or more ligands is facilitated by an additional level of control.[40,60,61] For this study, we chose octahedrally coordinated cobalt cations and embedded them in a large, dynamic-covalently closed salphen macrocycle ("$\mathbf{P}_2\mathbf{A}_2$"), consisting of two organic bridges between the two metal centers. The salphen moieties saturate four equatorial coordination sites per cobalt ion, allowing us to install two further bridging ligands "**E**" of appropriate length to complement a 3-dimensional cage structure without risking to form homoleptic species (Figure 3).

Cobalt was chosen as metal center here, because it allows to be introduced as kinetically labile Co(II) during the assembly phase. It can then be easily converted into Co(III) by aerobic oxidation, giving diamagnetic octahedral complexes with a diminished ligand exchange rate.[64] It is worth noting, that Akine and co-workers have endeavored a similar approach, recently, generating much smaller cavities than we report here.[65–68]

Ligand component **A** was synthesized by Suzuki cross-coupling of 2,7-dibromo-10-hexyl-9,9-dimethyl-9,10-dihydroacridine and 4-formyl-3-hydroxyphenylboronic acid pinacol ester. Macrocycle $\mathbf{P}_2\mathbf{A}_2$ was obtained in quantitative yields by an acid catalyzed condensation of **A** with *ortho*-phenylenediamine **P** in a 1:1 ratio (for synthetic details see the Supporting Information). The preparation of cage

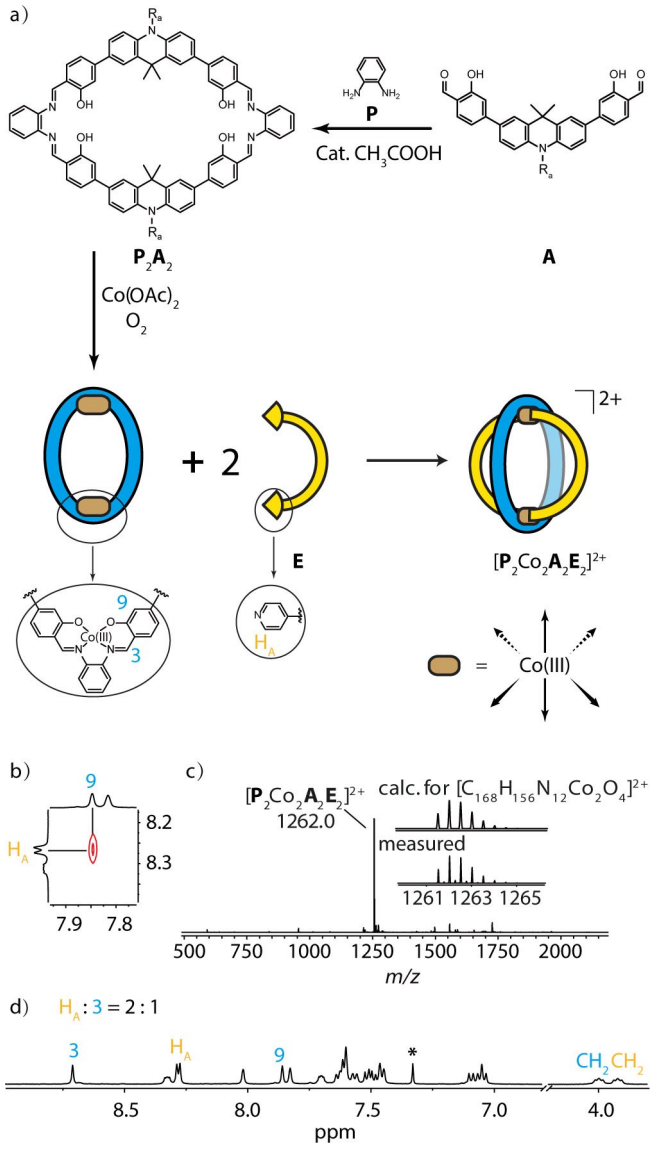

Figure 3. Synthesis of salphen-based macrocycle $\mathbf{P_2A_2}$ and heteroleptic cage $[\mathbf{P_2Co_2A_2E_2}]^{2+}$. a) Assembly scheme; b) ^{1}H-^{1}H NOESY NMR detail showing a cross signal between macrocycle $\mathbf{P_2A_2}$ and ligands **E**; c) high-resolution mass spectrum with calculated and observed isotope patterns of $[\mathbf{P_2Co_2A_2E_2}]^{2+}$; d) ^{1}H NMR spectrum (500 MHz) measured in CD_2Cl_2 (for details see Supporting Information).

$[\mathbf{P_2Co_2A_2E_2}]^{2+}$ required vigorous stirring of $Co(OAc)_2$ and ring $\mathbf{P_2A_2}$ for 15 mins in an acetonitrile-chloroform mixture ($v/v = 1:1$), followed by addition of ligand **E** and heating of the solution to 60 °C overnight under aerobic conditions. Subsequently, pure cage $[\mathbf{P_2Co_2A_2E_2}]^{2+}$ was precipitated as a dark red powder in 90 % isolated yield (Figure 3). The ^{1}H NMR characterization of $[\mathbf{P_2Co_2A_2E_2}]^{2+}$ revealed a single species featuring signals stemming from the **A** and **E** substructures in a 1:1 ratio (Figures S21–S24). Evidence for both ligands being integral components of the same supramolecular assembly came from an ^{1}H–^{1}H NOESY experiment, showing a clear cross-signal between proton *9* of the $\mathbf{P_2A_2}$ macrocycle and proton H_A of the bis-pyridyl ligands **E**, indicating a close intra-assembly contact. A DOSY NMR measurement confirmed that all proton signals assigned to $[\mathbf{P_2Co_2A_2E_2}]^{2+}$ feature the same diffusion coefficient (Figure S25). The high-resolution ESI-TOF mass spectrum of the compound showed a single, strong signal at $m/z = 1262.0$ for a 2+ species which is in excellent agreement with the calculated mass for formula $[\mathbf{P_2Co_2A_2E_2}]^{2+}$ (Figure S26). Slow vapor diffusion of ethyl acetate into a solution of $[\mathbf{P_2Co_2A_2E_2}]^{2+}$ in DMSO afforded red single crystals that were subjected to synchrotron radiation to yield diffraction data that allowed the determination of the solid-state structure (Figure 5a–c). Indeed, compound $[\mathbf{P_2Co_2A_2E_2}]^{2+}$ is a C_2-symmetric heteroleptic cage in which the bimetallic macrocycle (Co–Co distance = 14.2 Å) is bridged on both faces by banana-shaped **E**, filling the axial coordination sites of the Co(III) cations. The geminal methyl groups on macrocycle $\mathbf{P_2A_2}$ point to opposite directions (Figure 5c), giving it a slightly twisted conformation, but allowing the octahedral complexes to place the salphen's square-planar N_2O_2 environments in an almost co-planar orientation. Hence, two units of ligand **E** can bridge the axial positions of the cobalt centers from both sides (Figure 5b).

Heteroleptic cage $[P_2Co_2A_2BD]^{2+}$

When analyzing the structure of macrocyclic fragment $[\mathbf{P_2Co_2A_2}(dmso)_4]^{2+}$ by means of molecular modeling, two energetically almost degenerate conformations are obtained. In one case, the ring is slightly twisted with axial substituents protruding from both metal centers in a co-parallel fashion (as observed in the crystal structure of cage $[\mathbf{P_2Co_2A_2E_2}]^{2+}$, Figure 5a–c).

In the other case, the ring is bent like a crescent moon, suggesting that the axial coordination sites can be saturated by a pair of different bridging ligands, a longer one with converging donor sites and a shorter one with a diverging set of donors. We realized this situation to share similarity with our previously reported shape-complementarity approach, which allows the clean assembly of heteroleptic, *cis*-configured $[Pd_2L_2L'_2]$ cages from a set of two matching ligands and Pd(II) cations.[52,53] This prompted us to examine the combination of macrocyclic fragment $[\mathbf{P_2Co_2A_2}]^{2+}$ with pairs of donors of complementary shape and size (Figure 6). Pleasingly, the reaction of fluorene-based ligand **B** and carbazole-derived ligand **D** with macrocycle $\mathbf{P_2A_2}$ and $Co(OAc)_2$ under aerobic conditions, followed by precipitation, produced heteroleptic assembly $[\mathbf{P_2Co_2A_2BD}]^{2+}$ in 79 % isolated yield (Figure 4). ^{1}H NMR analysis showed significant downfield shifts for pyridyl protons H_a of **B** and H_I of **D**, indicative of the formation of coordination bonds to the Co(III) centers. In contrast, pyridyl protons H_b of **B** and H_{II} of **D** were found to shift upfield, satisfactorily explained by their positioning on top of the salphen phenylene units (Figure S29). Moreover, NMR signal integration of protons assigned to $\mathbf{P_2A_2}$, **B**, and **D** show a ratio of 2:1:1, thus matching the result expected for $[\mathbf{P_2Co_2A_2BD}]^{2+}$ (Figure 4d). In the NOESY NMR spectrum,

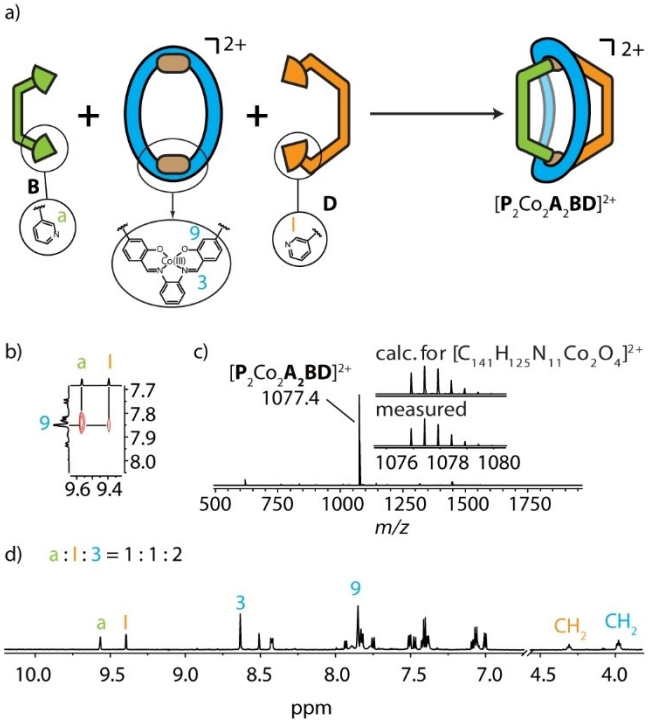

Figure 4. Synthesis of heteroleptic cage $[\mathbf{P}_2Co_2\mathbf{A}_2\mathbf{BD}]^{2+}$. a) Assembly scheme; b) ^{1}H-^{1}H NOESY NMR detail showing two cross signals between macrocycle $\mathbf{P}_2\mathbf{A}_2$ and ligands **B** and **D**; c) high-resolution mass spectrum with calculated and observed isotope patterns of $[\mathbf{P}_2Co_2\mathbf{A}_2\mathbf{BD}]^{2+}$; d) ^{1}H NMR spectrum (700 MHz) measured in CD_2Cl_2 (for details see Supporting Information).

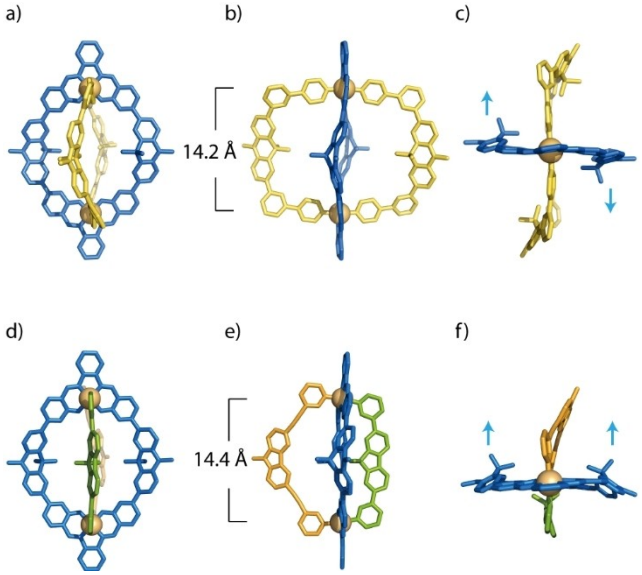

Figure 5. X-ray crystal structures of $[\mathbf{P}_2Co_2\mathbf{A}_2\mathbf{E}_2]^{2+}$ and $[\mathbf{P}_2Co_2\mathbf{A}_2\mathbf{BD}]^{2+}$. Front, side, and top views of the single crystal X-ray structures of a)–c), heteroleptic $[\mathbf{P}_2Co_2\mathbf{A}_2\mathbf{E}_2]^{2+}$ and d)–f), $[\mathbf{P}_2Co_2\mathbf{A}_2\mathbf{BD}]^{2+}$ (hydrogen atoms, counterions, and side chains were omitted for the clarity).

clear evidence for the intimate connection of all three organic components came from the observation of cross-peaks between macrocycle $\mathbf{P}_2\mathbf{A}_2$ and both ligand **B** and ligand **D**, respectively (Figure 4b). DOSY NMR analysis revealed that all proton signals assigned to $\mathbf{P}_2\mathbf{A}_2$, **B** and **D** belong to a single species with a hydrodynamic radius of 21.9 Å (Figure S32). The ESI-TOF mass spectrum virtually shows only a single peak at $m/z = 1077.4$ in the mass range between m/z 500 and 3000 which is in excellent agreement with the expected value and isotopic pattern for $[\mathbf{P}_2Co_2\mathbf{A}_2\mathbf{BD}]^{2+}$ (Figure 4c).

Single crystals suited for X-ray diffraction were obtained from DCM/ethyl acetate, yielding the structure shown in Figure 5d–f. As in the structure of $[\mathbf{P}_2Co_2\mathbf{A}_2\mathbf{E}_2]^{2+}$, the Co(III) cations adopt a typical octahedral geometry with two oxygen and two nitrogen donors from the $\mathbf{P}_2\mathbf{A}_2$ salphen ring filling the equatorial planes. As designed, the entire ring is slightly bent with the axial bonding vectors deviating from the horizontal that is orthogonal to the Co–Co axis, intersecting with an angle α of 19° (Figure S69). In contrast to the situation observed in the structure of $[\mathbf{P}_2Co_2\mathbf{A}_2\mathbf{E}_2]^{2+}$, the geminal methyl groups on macrocycle $\mathbf{P}_2\mathbf{A}_2$ of $[\mathbf{P}_2Co_2\mathbf{A}_2\mathbf{BD}]^{2+}$ now point in the same direction (Figure 5f). The shape-complementary bis-pyridyl ligands **B** and **D** perfectly follow the silhouette of the bent macrocycle $\mathbf{P}_2\mathbf{A}_2$ with shorter **B** binding on the concave side of the ring and longer **D** spanning over the convex face. We conducted first host–guest NMR titration experiments with cage $[\mathbf{P}_2Co_2\mathbf{A}_2\mathbf{BD}]^{2+}$. While double negatively charged sulfonate guests resulted in instantaneous precipitation with the di-cationic cage, titration with mono-anionic organic sulfonates caused some of the cage's proton signals to shift, thus indicating interaction between the cage interior and/or periphery and these guest molecules (Figures S34, S35).

Further Assembly Studies

In order to obtain a deeper understanding of the factors governing the self-assembly of the heteroleptic cages, we performed a number of experiments. First of all, we evaluated how the bis-pyridyl ligands **B**, **D** and **E** behave when combined with square-planar Pd(II) cations. Unsurprisingly, the reaction of **E** with $[Pd(CH_3CN)_4](BF_4)_2$ in a 2:1 ratio in acetonitrile results in the quantitative formation of cage $[Pd_2\mathbf{E}_4]^{4+}$. Figure 6a shows its single crystal X-ray structure (for NMR and HRMS analysis, see the Supporting Information). Interestingly, a 1:1:1 mixture of ligands **B** and **D** with the same Pd(II) precursor, reacted in CD_3CN at 70 °C overnight, yields heteroleptic cage *cis*-$[Pd_2\mathbf{B}_2\mathbf{D}_2]^{4+}$ which was fully characterized by NMR, HR-MS[59,61,69] and – now for the first time – single crystal analysis (Figure 6b, details see the Supporting Information). When comparing the X-ray structures of $[Pd_2\mathbf{B}_2\mathbf{D}_2]^{4+}$ and $[\mathbf{P}_2Co_2\mathbf{A}_2\mathbf{BD}]^{2+}$, both comprising ligands **B** and **D** in a 1:1 fashion, a remarkable geometrically consistency was observed. Angle β, formed between the two Pd(pyridine)$_4$ planes of $[Pd_2\mathbf{B}_2\mathbf{D}_2]^{4+}$ is with 21° almost equal to angle $\alpha = 19°$ of cage $[\mathbf{P}_2Co_2\mathbf{A}_2\mathbf{BD}]^{2+}$. In addition, the observed Pd–Pd distance (13.6 Å) is also quite close to the Co–Co distance (14.4 Å, see Table S4).

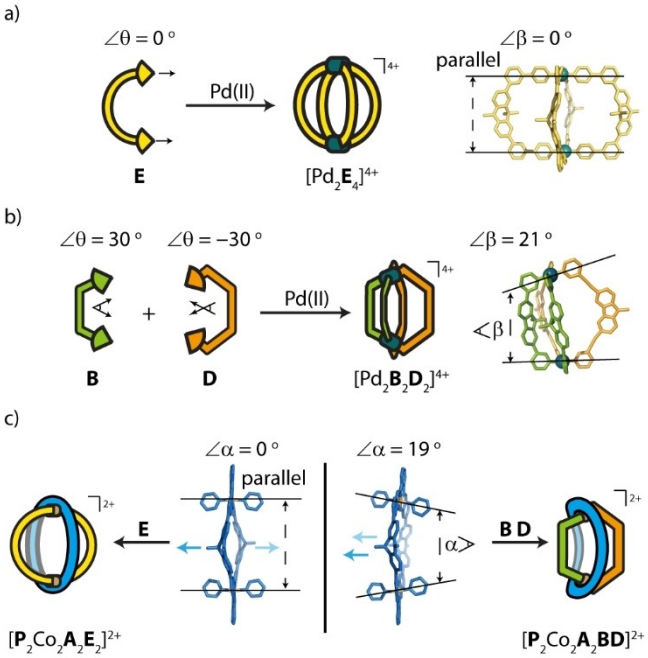

Figure 6. Comparison of selected X-ray structural features. a) Parallel coordination vectors in homoleptic $[Pd_2\mathbf{E}_4]^{4+}$; b) shape-complementary formation of bent cage $[Pd_2\mathbf{B}_2\mathbf{D}_2]^{4+}$; c) the twisted conformation of ring $\mathbf{P}_2\mathbf{A}_2$ leads to parallel vectors in $[\mathbf{P}_2Co_2\mathbf{A}_2\mathbf{E}_2]^{2+}$ while the crescent-shaped conformer of $\mathbf{P}_2\mathbf{A}_2$ leads to tilted vectors, perfectly matching the angles of **B** and **D** in $[\mathbf{P}_2Co_2\mathbf{A}_2\mathbf{BD}]^{2+}$.

Next, we tackled the question whether the selective formation of heteroleptic Co(III)-based cages is kinetically controlled or thermodynamically driven. Therefore, we performed a self-sorting experiment (Figure S54): Two flasks were charged with the same amount of macrocycle $\mathbf{P}_2\mathbf{A}_2$ (1.0 eq.) and $Co(OAc)_2$ (2.0 eq.) in DMSO. After adding 2.0 eq. of either **B** or **D**, the mixtures were heated under air atmosphere to 70 °C for 19 h. Results were examined by high-resolution mass spectrometry. In the sample containing **D**, a statistical mixture with up to four counts of **D** coordinated to fragment $[\mathbf{P}_2Co_2\mathbf{A}_2]^{2+}$ was observed, indicating that ligand **D** alone has a poor geometric complementarity with the macrocycle to form a defined $[\mathbf{P}_2Co_2\mathbf{A}_2\mathbf{D}_2]^{2+}$ cage structure. Where **B** was added, only complexes with up to three units of **B** were observed, indicating that one molecule of **B** readily bridges the bent conformation of $[\mathbf{P}_2Co_2\mathbf{A}_2]^{2+}$ to form fragment $[\mathbf{P}_2Co_2\mathbf{A}_2\mathbf{B}]^{2+}$ while two additional ligands **B** coordinate to the other face in a dangling mode. Next, we mixed the two samples in a ratio of 1:1 and heated at 70 °C for 24 h, again giving cage $[\mathbf{P}_2Co_2\mathbf{A}_2\mathbf{BD}]^{2+}$ as the major product, thus supporting that its formation is thermodynamically driven.

A series of DFT geometry optimizations were performed to learn about the relative energetics of cage formation according to the simplified scheme: $[\mathbf{P}_2Co_2\mathbf{A}_2(DMSO)_4]^{2+} + 2\,L \rightarrow [\mathbf{P}_2Co\mathbf{A}_2L_2]^{2+} + 4$ DMSO (L = **B**, **D** or **E**; neglecting solvent and counter anion effects, Table S1). Results indicate that the formation of $[\mathbf{P}_2Co_2\mathbf{A}_2\mathbf{BD}]^{2+}$ from its components is energetically much more favorable than reactions leading to tentative complexes $[\mathbf{P}_2Co_2\mathbf{A}_2\mathbf{B}_2]^{2+}$ (by about 50 kJ/mol) and $[\mathbf{P}_2Co_2\mathbf{A}_2\mathbf{D}_2]^{2+}$ (by about 30 kJ/mol). Interestingly, cage $[\mathbf{P}_2Co_2\mathbf{A}_2\mathbf{E}_2]^{2+}$, consisting of the macrocycle and two identical made-to-fit ligands, is formed with an even higher energetic preference (Supporting Information).

Heteroleptic Cage $[P_2Co_2ABCD]^{2+}$

Finally, we pursued the rational synthesis of target compound $[\mathbf{P}_2Co_2\mathbf{ABCD}]^{2+}$ (Figure 7). Therefore, the literature-known possibility to prepare non-symmetric salen/salphen complexes[70,71] was utilized to assemble dinuclear ring $[\mathbf{P}_2Co_2\mathbf{AC}]^{2+}$ ring with broken symmetry in which **A** carries an *n*-hexyl chain, while **C** is equipped with a 3,6-dioxaheptyl appendix (Figure 7a).

As a precursor to unsymmetric $[Co_2\mathbf{AC}]^{2+}$, half-macrocycle **A′** (=$\mathbf{P}_2\mathbf{A}$) was synthesized in quantitative yields by condensing the salicylic aldehyde precursor with *ortho*-phenylene diamine **P** under carefully controlled conditions (Supporting Information). Cage $[\mathbf{P}_2Co_2\mathbf{ABCD}]^{2+}$ was then produced by a one-pot, five component self-assembly: organic bridges **A′**, **B**, **C** and **D** were mixed in DMSO, $Co(acetate)_2$ added and the reaction stirred at 60 °C under N_2 atmosphere overnight. Subsequently, NH_4PF_6 was added and the reaction mixture was exposed to air for one further hour to finish the reaction. After purification by three precipitation rounds, 57 % isolated yield were obtained. To gain deeper insight into the process, we repeated the synthesis step by step. Unlike macrocycle $\mathbf{P}_2\mathbf{A}_2$, pure $\mathbf{P}_2\mathbf{AC}$ can hardly be produced, as shuffling to a mixture of $\mathbf{P}_2\mathbf{A}_2$, $\mathbf{P}_2\mathbf{AC}$ and $\mathbf{P}_2\mathbf{C}_2$, occurs. Upon mixing fragments **A′** and **C** in the presence of $Co(OAc)_2$ in a ratio of 1:1:2 in DMSO, however, complex $[\mathbf{P}_2Co_2\mathbf{AC}]^{2+}$ was identified as the only intermediate (Figure S42), with the cobalt cations most probably acting as templates. Subsequent addition of **B**, **D** and NH_4PF_6 provided heteroleptic cage $[\mathbf{P}_2Co_2\mathbf{ABCD}]^{2+}$ in decent yields. NMR analysis confirmed the successful formation of the target compound containing non-symmetric macrocycle $\mathbf{P}_2\mathbf{AC}$, exclusively. For example, whereas proton *3* in $[\mathbf{P}_2Co_2\mathbf{A}_2\mathbf{BD}]^{2+}$ gave rise to one singlet at 8.63 ppm (Figure S37), compound $[\mathbf{P}_2Co_2\mathbf{ABCD}]^{2+}$ features two singlets as a consequence of the reduced symmetry (Figure 7d). Again, the NOESY NMR spectrum shows clear cross signals between macrocycle $\mathbf{P}_2\mathbf{AC}$ and ligands **B** and **D** (Figure 7b). DOSY NMR analysis revealed that all signals belonging to bridges **A**, **B**, **C**, **D** correspond to the same diffusion coefficient (Figure S40). The ESI-MS analysis shows a single signal at $m/z = 1086.4$, in perfect agreement with the formula $[\mathbf{P}_2Co_2\mathbf{ABCD}]^{2+}$ (Figure 7c). In addition, we were able to distinguish cages $[\mathbf{P}_2Co_2\mathbf{ABCD}]^{2+}$ and $[\mathbf{P}_2Co_2\mathbf{A}_2\mathbf{BD}]^{2+}$ by co-injecting them into a trapped ion mobility spectrometer, coupled to high-resolution ESI mass spectrometry (ESI-timsTOF), giving collisional cross section (CCS) values of 557.8 Å^2 and 562.8 Å^2, respectively (Figure S44).[57] Finally, the structure of $[\mathbf{P}_2Co_2\mathbf{ABCD}]^{2+}$ was confirmed by single crystal X-ray analysis. Red plate-shaped crystals were produced by layering ethyl acetate on top of a solution of

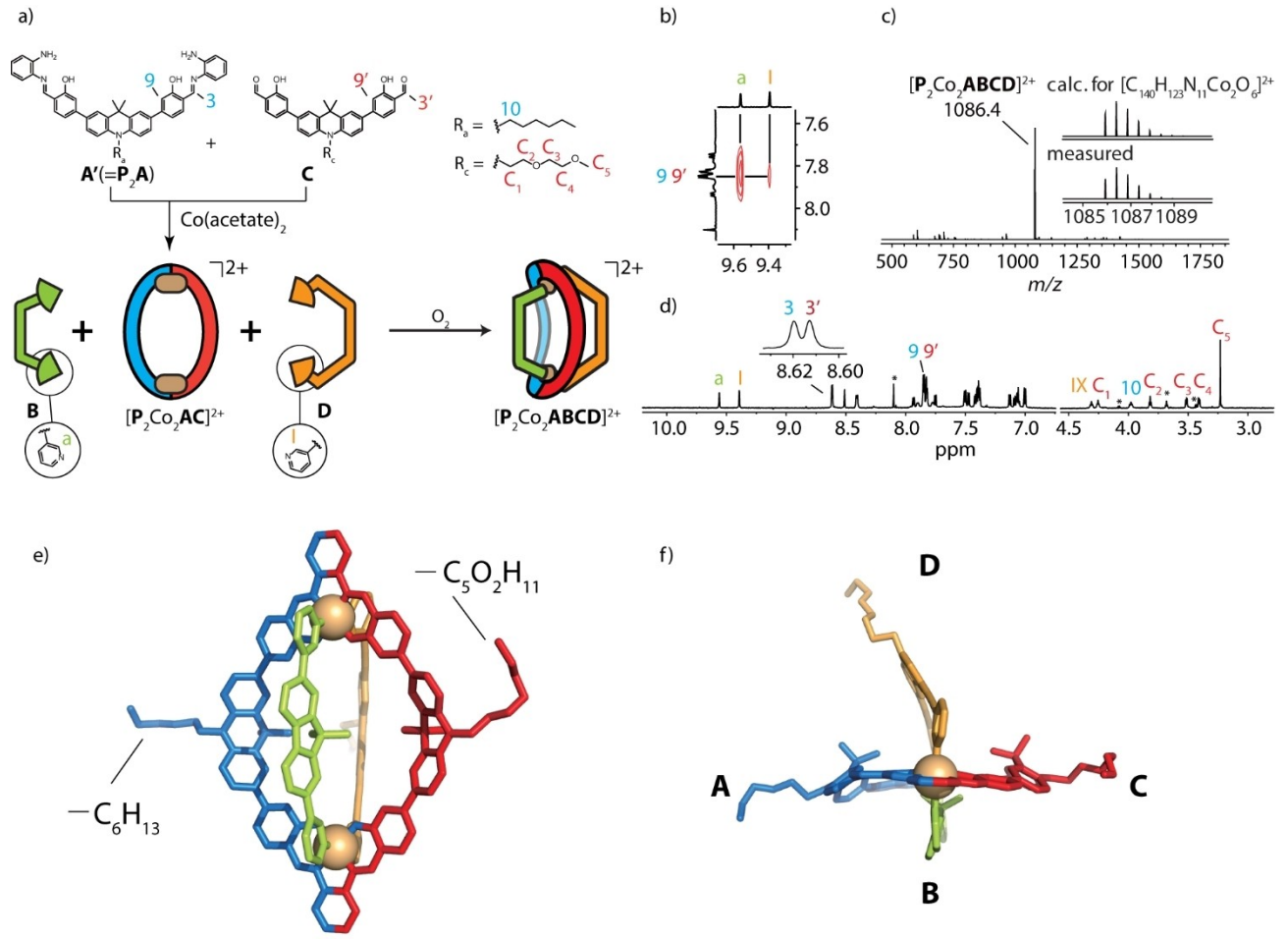

Figure 7. Self-assembly of heteroleptic cage $[\mathbf{P_2Co_2ABCD}]^{2+}$. a) Assembly scheme; b) ^{1}H-^{1}H NOESY NMR detail showing cross signals between macrocycle $\mathbf{P_2AC}$ and ligands **B** and **D**; c) high-resolution mass spectrum with calculated and observed isotope patterns; d) ^{1}H NMR spectrum (700 MHz) measured in CD_2Cl_2; e) and f) front and top views of the single crystal X-ray structure of heteroleptic $[\mathbf{P_2Co_2ABCD}]^{2+}$ (hydrogen atoms and counterions were omitted for clarity).

$[\mathbf{P_2Co_2ABCD}]^{2+}$ in DCM. The structure of complex $[\mathbf{P_2Co_2ABCD}]^{2+}$ is shown in Figure 7e–f. While it is very similar to the structure of cage $[\mathbf{P_2Co_2A_2BD}]^{2+}$, the two different halves of ring $\mathbf{P_2AC}$ could be distinguished in the X-ray structure result by matching the different lengths of the appended chains to the observed electron density (Supporting Information).

Conclusion

Artificial host compounds with nano-sized cavities can be prepared by covalent synthesis or dynamic (non-)covalent self-assembly. While the first approach does allow desymmetrization and multifunctionalization of highly stable organic host structures,[23,25] this may require a series of tedious synthesis and purification steps. Self-assembly can serve as elegant alternative, but the rational combination of multiple different building blocks without risking to generate convoluted libraries is challenging and the so far reported Pd(II) structures are of rather dynamic nature.[40,56–61] Here, we combine the macrocyclization of two salphen chelate environments with the rational introduction of two shape-complementary bridges, filling the axial positions of octahedrally coordinated cobalt cations. High self-sorting fidelity is achieved by introducing the metal centers in the form kinetically labile Co(II) ions, while subsequent aerobic oxidation stabilizes the assemblies through the generation of octahedral low-spin d^6 Co(III) nodes. This allowed us to direct the assembly of a series of heteroleptic cage structures, featuring up to four different organic bridges, from a one-pot mixture of four tailored building blocks and one metal precursor.[72] While these prototype cages were designed without dedicated functionality in the backbones, the strategy has potential to equip a following generation of Co(III)salphen-based heteroleptic cages and other supramolecular architectures with a modular combination of different, precisely arranged functions such as chiral information carriers, photo-redox centers, selective recognition and catalytic sites –challenges that we are currently pursuing.

Supporting Information

The authors have cited additional references within the Supporting Information.[73–86]

Acknowledgements

We thank Dr. Andreas Brockmeyer and Christiane Heitbrink (Max-Planck Institute for Molecular Physiology, Dortmund), Dr. Holm Frauendorf (Georg-August University Göttingen), Dr. David Engelhard and Laura Schneider (TU Dortmund) for mass spectrometry measurements and Prof. Dr. Wolf Hiller, Dr. André Platzek and Dr. Jacopo Tessarolo (TU Dortmund) for support with NMR measurements, Dr. Christina Krabbe for formatting and Laura Neukirch for the German translation. Diffraction data of $[\mathbf{P}_2Co_2\mathbf{A}_2\mathbf{E}_2](PF_6)_2$, $[\mathbf{P}_2Co_2\mathbf{A}_2\mathbf{BD}](PF_6)_2$, $[\mathbf{P}_2Co_2\mathbf{ABCD}](PF_6)_2$ and $[Pd_2\mathbf{B}_2\mathbf{D}_2](BF_4)_4$ were collected at PETRA III at DESY, a member of the Helmholtz Association (HGF).[72] We thank Anja Burkhardt, Saravanan Panneerselvam and Sebastian Guenther for assistance in using synchrotron beamline P11 (I-20160736, I-20170404 and I-20170714). We thank the European Research Council (ERC Consolidator grant 683083, RAMSES) and the Deutsche Forschungsgemeinschaft (DFG priority program SPP 1807 "Control of London Dispersion Interactions in Molecular Chemistry", project CL 489/3-2) for financial support. This work was supported by grants of the National Research Foundation of Korea, funded by the Korean Government (NRF-2018R1A6A3A03012675 and NRF-2021R1C1C1013037). Open Access funding enabled and organized by Projekt DEAL.

Conflict of Interest

The authors declare no conflict of interest.

Data Availability Statement

The data that support the findings of this study are available from the corresponding author upon reasonable request.

Keywords: Cobalt · Self-Assembly · Cages · Coordination Chemistry · Supramolecular Chemistry

[1] R. Chakrabarty, P. S. Mukherjee, P. J. Stang, *Chem. Rev.* **2011**, *111*, 6810–918.
[2] M. Fujita, M. Tominaga, A. Hori, B. Therrien, *Acc. Chem. Res.* **2005**, *38*, 369–378.
[3] M. M. J. Smulders, I. A. Riddell, C. Browne, J. R. Nitschke, *Chem. Soc. Rev.* **2012**, *42*, 1728–1754.
[4] M. Han, D. M. Engelhard, G. H. Clever, *Chem. Soc. Rev.* **2014**, *43*, 1848–1860.
[5] D. J. Tranchemontagne, Z. Ni, M. O'Keeffe, O. M. Yaghi, *Angew. Chem. Int. Ed.* **2008**, *47*, 5136–5147.
[6] S. Kitagawa, R. Kitaura, S. Noro, *Angew. Chem. Int. Ed.* **2004**, *43*, 2334–2375.
[7] H. Wang, X. Qian, K. Wang, M. Su, W.-W. Haoyang, X. Jiang, R. Brzozowski, M. Wang, X. Gao, Y. Li, B. Xu, P. Eswara, X.-Q. Hao, W. Gong, J.-L. Hou, J. Cai, X. Li, *Nat. Commun.* **2018**, *9*, 1815.
[8] T. Zhang, L.-P. Zhou, X.-Q. Guo, L.-X. Cai, Q.-F. Sun, *Nat. Commun.* **2017**, *8*, 15898.
[9] I. A. Riddell, M. M. J. Smulders, J. K. Clegg, Y. R. Hristova, B. Breiner, J. D. Thoburn, J. R. Nitschke, *Nat. Chem.* **2012**, *4*, 751.
[10] V. Brega, M. Zeller, Y. He, H. P. Lu, J. K. Klosterman, *Chem. Commun.* **2015**, *51*, 5077–5080.
[11] N. Kishi, Z. Li, K. Yoza, M. Akita, M. Yoshizawa, *J. Am. Chem. Soc.* **2011**, *133*, 11438–11441.
[12] T. Beissel, R. E. Powers, K. N. Raymond, *Angew. Chem. Int. Ed.* **1996**, *35*, 1084–1086.
[13] T. Brasey, R. Scopelliti, K. Severin, *Chem. Commun.* **2006**, 3308–3310.
[14] S. Pasquale, S. Sattin, E. C. Escudero-Adán, M. Martínez-Belmonte, J. de Mendoza, *Nat. Commun.* **2012**, *3*, 785.
[15] Q.-F. Sun, S. Sato, M. Fujita, *Nat. Chem.* **2012**, *4*, 330.
[16] I. A. Bhat, D. Samanta, P. S. Mukherjee, *J. Am. Chem. Soc.* **2015**, *137*, 9497–9502.
[17] D. Fujita, Y. Ueda, S. Sato, N. Mizuno, T. Kumasaka, M. Fujita, *Nature* **2016**, *540*, 563.
[18] M. D. Ward, C. A. Hunter, N. H. Williams, *Acc. Chem. Res.* **2018**, *51*, 2073–2082.
[19] J. A. Davies, T. K. Ronson, J. R. Nitschke, *Chem* **2022**, *8*, 1099–1106.
[20] K. Wu, T. K. Ronson, P. Su, Z. Chen, L. Goh, A. W. Heard, X. Li, F. Klautzsch, C. A. Schalley, M. Vinković, J. R. Nitschke, *Nat. Synth.* **2023**, *2*, 789–797.
[21] Y.-S. Chen, E. Solel, Y.-F. Huang, C.-L. Wang, T.-H. Tu, E. Keinan, Y.-T. Chan, *Nat. Commun.* **2019**, *10*, 3443.
[22] S. Klotzbach, F. Beuerle, *Angew. Chem. Int. Ed.* **2015**, *54*, 10356–10360.
[23] M. Otte, M. Lutz, R. J. M. K. Gebbink, *Eur. J. Org. Chem.* **2017**, *2017*, 1657–1661.
[24] N. Christinat, R. Scopelliti, K. Severin, *Angew. Chem. Int. Ed.* **2008**, *47*, 1848–1852.
[25] S. C. Bete, M. Otte, *Angew. Chem. Int. Ed.* **2021**, *60*, 18582–18586.
[26] L. A. Wessjohann, O. Kreye, D. G. Rivera, *Angew. Chem. Int. Ed.* **2017**, *56*, 3501–3505.
[27] Z. He, W. Jiang, C. A. Schalley, *Chem. Soc. Rev.* **2014**, *44*, 779–789.
[28] S. Pullen, G. H. Clever, *Acc. Chem. Res.* **2018**, *51*, 3052–3064.
[29] S. Pullen, J. Tessarolo, G. H. Clever, *Chem. Sci.* **2021**, *12*, 7269–7293.
[30] T. K. Ronson, D. A. Roberts, S. P. Black, J. R. Nitschke, *J. Am. Chem. Soc.* **2015**, *137*, 14502–14512.
[31] Y. Yang, T. K. Ronson, D. Hou, J. Zheng, I. Jahović, K. H. Luo, J. R. Nitschke, *J. Am. Chem. Soc.* **2023**, *145*, 19164–19170.
[32] T. K. Ronson, J. P. Carpenter, J. R. Nitschke, *Chem* **2022**, *8*, 557–568.
[33] M. Yamashina, T. Yuki, Y. Sei, M. Akita, M. Yoshizawa, *Chem. Eur. J.* **2015**, *21*, 4200–4204.
[34] D. Preston, J. E. Barnsley, K. C. Gordon, J. D. Crowley, *J. Am. Chem. Soc.* **2016**, *138*, 10578–85.
[35] Y.-R. Zheng, Z. Zhao, M. Wang, K. Ghosh, J. B. Pollock, T. R. Cook, P. J. Stang, *J. Am. Chem. Soc.* **2010**, *132*, 16873–82.
[36] M. Yoshizawa, M. Nagao, K. Kumazawa, M. Fujita, *J. Organomet. Chem.* **2005**, *690*, 5383–5388.
[37] V. Maurizot, M. Yoshizawa, M. Kawano, M. Fujita, *Dalton Trans.* **2006**, 2750–2756.
[38] R. Zhu, W. M. Bloch, J. J. Holstein, S. Mandal, L. V. Schäfer, G. H. Clever, *Chem. Eur. J.* **2018**, *24*, 12976–12982.

[39] B. Chen, J. J. Holstein, A. Platzek, L. Schneider, K. Wu, G. H. Clever, *Chem. Sci.* **2022**, *13*, 1829–1834.
[40] Y. Liu, S. Liao, W. Dai, Q. Bai, S. Lu, H. Wang, X. Li, Z. Zhang, P. Wang, W. Lu, Q. Zhang, *Angew. Chem. Int. Ed.* **2023**, *62*, e202217215.
[41] P. Molinska, A. Tarzia, L. Male, K. E. Jelfs, J. E. M. Lewis, *Angew. Chem. Int. Ed.* **2023**, *62*, e202315451.
[42] R.-J. Li, J. Tessarolo, H. Lee, G. H. Clever, *J. Am. Chem. Soc.* **2021**, *143*, 3865–3873.
[43] J. E. M. Lewis, *Angew. Chem. Int. Ed.* **2022**, *61*, e202212392.
[44] C. García-Simón, R. Gramage-Doria, S. Raoufmoghaddam, T. Parella, M. Costas, X. Ribas, J. N. H. Reek, *J. Am. Chem. Soc.* **2015**, *137*, 2680–2687.
[45] Q. Sun, S. Sato, M. Fujita, *Angew. Chem. Int. Ed.* **2014**, *53*, 13510–13513.
[46] J. A. Davies, T. K. Ronson, J. R. Nitschke, *J. Am. Chem. Soc.* **2024**, *146*, 5215–5223.
[47] S. Mukherjee, P. S. Mukherjee, *Chem. Commun.* **2014**, *50*, 2239–2248.
[48] P. Howlader, P. Das, E. Zangrando, P. S. Mukherjee, *J. Am. Chem. Soc.* **2016**, *138*, 1668–1676.
[49] S. Prusty, K. Yazaki, M. Yoshizawa, D. K. Chand, *Chem. Eur. J.* **2017**, *23*, 12456–12461.
[50] J.-R. Li, H.-C. Zhou, *Nat. Chem.* **2010**, *2*, 893.
[51] S.-C. Li, L.-X. Cai, M. Hong, Q. Chen, Q.-F. Sun, *Angew. Chem. Int. Ed.* **2022**, *61*, e202204732.
[52] W. M. Bloch, Y. Abe, J. J. Holstein, C. M. Wandtke, B. Dittrich, G. H. Clever, *J. Am. Chem. Soc.* **2016**, *138*, 13750–13755.
[53] W. M. Bloch, J. J. Holstein, W. Hiller, G. H. Clever, *Angew. Chem. Int. Ed.* **2017**, *56*, 8285–8289.
[54] S. Gaikwad, M. L. Saha, D. Samanta, M. Schmittel, *Chem. Commun.* **2017**, *53*, 8034–8037.
[55] M. L. Saha, M. Schmittel, *Inorg. Chem.* **2016**, *55*, 12366–12375.
[56] W. M. Bloch, G. H. Clever, *Chem. Commun.* **2017**, *53*, 8506–8516.
[57] K. E. Ebbert, L. Schneider, A. Platzek, C. Drechsler, B. Chen, R. Rudolf, G. H. Clever, *Dalton Trans.* **2019**, *48*, 11070–11075.
[58] D. Preston, J. D. Evans, *Angew. Chem. Int. Ed.* **2023**, e202314378.
[59] E. Benchimol, I. Regeni, B. Zhang, M. Kabiri, J. J. Holstein, G. H. Clever, *J. Am. Chem. Soc.* **2024**, *146*, 6905–6911.
[60] T. Abe, N. Sanada, K. Takeuchi, A. Okazawa, S. Hiraoka, *J. Am. Chem. Soc.* **2023**, *145*, 28061–28074.
[61] K. Wu, E. Benchimol, A. Baksi, G. H. Clever, *Nat. Chem.* **2024**, DOI: 10.1038/s41557-023-01415-7.
[62] S. Samantray, S. Krishnaswamy, D. K. Chand, *Nat. Commun.* **2020**, *11*, 880.
[63] L.-J. Chen, H.-B. Yang, *Acc. Chem. Res.* **2018**, *51*, 2699–2710.
[64] P. R. Symmers, M. J. Burke, D. P. August, P. I. T. Thomson, G. S. Nichol, M. R. Warren, C. J. Campbell, P. J. Lusby, *Chem. Sci.* **2014**, *6*, 756–760.
[65] S. Akine, M. Miyashita, T. Nabeshima, *J. Am. Chem. Soc.* **2017**, *139*, 4631–4634.
[66] Y. Sakata, C. Murata, S. Akine, *Nat. Commun.* **2017**, *8*, 16005.
[67] Y. Sakata, M. Tamiya, M. Okada, S. Akine, *J. Am. Chem. Soc.* **2019**, *141*, 15597–15604.
[68] Y. Sakata, M. Okada, S. Akine, *Chem. Eur. J.* **2021**, *27*, 2284–2288.
[69] K. Wu, B. Zhang, C. Drechsler, J. J. Holstein, G. H. Clever, *Angew. Chem. Int. Ed.* **2020**, *60*, 6403–6407.
[70] P. D. Frischmann, J. Jiang, J. K.-H. Hui, J. J. Grzybowski, M. J. MacLachlan, *Org. Lett.* **2008**, *10*, 1255–1258.
[71] A. M. Castilla, S. Curreli, E. C. Escudero-Adán, M. M. Belmonte, J. Benet-Buchholz, A. W. Kleij, *Org. Lett.* **2009**, *11*, 5218–21.
[72] Deposition Numbers 1903507 (for $[\mathbf{P}_2Co_2\mathbf{A}_2\mathbf{E}_2](PF_6)_2$), 1903508 (for $[\mathbf{P}_2Co_2\mathbf{A}_2\mathbf{BD}](PF_6)_2$), 1903509 (for $[Pd_2\mathbf{E}_4](BF_4)_4$), 1903510 (for $[Pd_2\mathbf{B}_2\mathbf{D}_2](BF_4)_4$), 1903511 (for $[\mathbf{P}_2Co_2\mathbf{ABCD}](PF_6)_2$) contain the supplementary crystallographic data for this paper. These data are provided free of charge by the joint Cambridge Crystallographic Data Centre and Fachinformationszentrum Karlsruhe Access Structures service.
[73] T. L. Andrew, T. M. Swager, *J. Org. Chem.* **2011**, *76*, 2976–2993.
[74] F. Mamiya, N. Ousaka, E. Yashima, *Angew. Chem. Int. Ed.* **2015**, *54*, 14442–14446.
[75] S.-J. Su, D. Tanaka, Y.-J. Li, H. Sasabe, T. Takeda, J. Kido, *Org. Lett.* **2008**, *10*, 941–944.
[76] R. Zhu, J. Lübben, B. Dittrich, G. H. Clever, *Angew. Chem. Int. Ed.* **2015**, *54*, 2796–2800.
[77] Spartan'08 Version 1.2.0, Wavefunction, Inc., Irvine, CA, USA **2009**.
[78] M. J. Frisch, G. W. Trucks, H. B. Schlegel, G. E. Scuseria, M. A. Robb, J. R. Cheeseman, G. Scalmani, V. Barone, G. A. Petersson, H. Nakatsuji, X. Li, M. Caricato, A. V. Marenich, J. Bloino, B. G. Janesko, R. Gomperts, B. Mennucci, H. P. Hratchian, J. V. Ortiz, A. F. Izmaylov, J. L. Sonnenberg, D. Williams-Young, F. Ding, F. Lipparini, F. Egidi, J. Goings, B. Peng, A. Petrone, T. Henderson, D. Ranasinghe, V. G. Zakrzewski, J. Gao, N. Rega, G. Zheng, W. Liang, M. Hada, M. Ehara, K. Toyota, R. Fukuda, J. Hasegawa, M. Ishida, T. Nakajima, Y. Honda, O. Kitao, H. Nakai, T. Vreven, K. Throssell, J. A. Montgomery Jr., J. E. Peralta, F. Ogliaro, M. J. Bearpark, J. J. Heyd, E. N. Brothers, K. N. Kudin, V. N. Staroverov, T. A. Keith, R. Kobayashi, J. Normand, K. Raghavachari, A. P. Rendell, J. C. Burant, S. S. Iyengar, J. Tomasi, M. Cossi, J. M. Millam, M. Klene, C. Adamo, R. Cammi, J. W. Ochterski, R. L. Martin, K. Morokuma, O. Farkas, J. B. Foresman, D. J. Fox, *Gaussian 09, Revision D.01*, Gaussian, Inc., Wallingford CT **2009**.
[79] A. Burkhardt, T. Pakendorf, B. Reime, J. Meyer, P. Fischer, N. Stübe, S. Panneerselvam, O. Lorbeer, K. Stachnik, M. Warmer, P. Rödig, D. Göries, A. Meents, *Eur. Phys. J. Plus* **2016**, *131*, 56.
[80] W. Kabsch, *Acta Crystallogr. Sect. D* **2010**, *66*, 125–132.
[81] G. M. Sheldrick, *Acta Crystallogr. Sect. A* **2015**, *71*, 3–8.
[82] G. M. Sheldrick, *Acta Crystallogr. Sect. C* **2015**, *71*, 3–8.
[83] C. B. Hübschle, G. M. Sheldrick, B. Dittrich, *J. Appl. Crystallogr.* **2011**, *44*, 1281–1284.
[84] A. Thorn, B. Dittrich, G. M. Sheldrick, *Acta Crystallogr. Sect. A* **2012**, *68*, 448–451.
[85] A. L. Spek, *Acta Crystallogr. Sect. C* **2015**, *71*, 9–18.
[86] A. L. Spek, *Acta Crystallogr. Sect. D* **2009**, *65*, 148–155.

Manuscript received: March 7, 2024
Accepted manuscript online: April 4, 2024
Version of record online: May 6, 2024